

SPATIOGRAM FEATURES TO CHARACTERIZE PEARLS IN PAINTINGS

L. Platiša,^a B. Cornelis,^b T. Ružić,^a A. Pižurica,^a A. Dooms,^b M. Martens,^c M. De Mey,^d I. Daubechies^e

^aGhent University, TELIN-IPI-IBBT, Ghent, Belgium;

^bVrije Universiteit Brussel, ETRO-IBBT, Brussels, Belgium;

^cGhent University, Faculty of Arts and Philosophy, Dept. of Art, Music and Theatre, Ghent, Belgium

^dThe Flemish Academic Centre for Science and the Arts (VLAC), Brussels, Belgium;

^eDuke University, Mathematics Department, Durham, NC, US

ABSTRACT

Objective characterization of jewels in paintings, especially pearls, has been a long lasting challenge for art historians. The way an artist painted pearls reflects his ability to observing nature and his knowledge of contemporary optical theory. Moreover, the painterly execution may also be considered as an individual characteristic useful in distinguishing hands. In this work, we propose a set of image analysis techniques to analyze and measure spatial characteristics of the digital images of pearls, all relying on the so called *spatiogram* image representation. Our experimental results demonstrate good correlation between the new metrics and the visually observed image features, and also capture the degree of realism of the visual appearance in the painting. In that sense, these results set the basis in creating a practical tool for art historical attribution and give strong motivation for further investigations in this direction.

Index Terms— Ghent Altarpiece, image analysis, histograms, spatiograms, content similarity

1. INTRODUCTION

In his 1435 treatise on the theory of painting *De pictura* (“On Painting”), Leon Battista Alberti remarks that “gems and all precious things of that kind become much more precious by the painter’s hand” [1]. Indeed, artists have been attracted to the beauty of precious stones and challenged to depict jewelery in their paintings for ages. As neatly reviewed by Autin *et al.* in the recent *Jewels in Painting* [2], the first pearls appear in the paintings of XVth-century artists. These include the *Portrait of a Young Lady* by Petrus Christus and the portrait of Queen Margaret of Denmark by Hugo Van der Goes, in Flanders, and the portrait of Simonetta Vespucci by Piero di Cosimo and the portrait of Battista Storza by Piero della Francesca, in Italy. Famous later examples include, of course, the depictions in Vermeer’s *Girl with the Pearl Earring* and Ingres’ *Turkish Bath*.

The way an artist painted pearls reflects his ability to observing nature, and in some cases like Jan Van Eyck, his knowledge of contemporary optical theory [3]. The painterly execution may also be considered as an idiosyncratic marker or an individual characteristic useful in distinguishing hands. In this context, our method aspires to creating a tool for art historical attribution.

We explore mathematical tools that could assist art historians in studying the jewels in paintings, all in the domain of digital image analysis. The proposed techniques are based on the image spatiograms [4] which extend the concept of histograms to the spatial domain. Knowing that surface reflectance is among the most notable

characteristics of the jewels in paintings, it was essential to have the spatial information involved in the analysis of pearl images.

Our contribution is threefold. Firstly, we demonstrate the ability of the spatiogram similarity metric to quantify the similarity between pearl images. Secondly, we introduce a method for matching spatiograms of the images. Thirdly, we propose a set of novel metrics built around the spatial characteristics of the image data. As we will show in the paper, these techniques can be used in multiple manners, including numerical quantification of the visually observed image features and the degree of realism of the visual appearance in the painting, characterization of the specific properties of rendering of different materials by an artist, or detecting copies of the artworks.

To test the performance of our proposed techniques we use both the images of painted pearls and those of photographed ones. For the pearls in paintings, we look at *The Ghent Altarpiece*, both the pearls painted by the original masters, the Van Eyck brothers (1432), and those of their copyists, Jef Van der Veken (1945) and Charlotte Caspers (2010). In addition, we consider the pearls painted by Hans Memling in his *Portrait of Maria Maddalena Baroncelli* (1470).

In the next section, we demonstrate the benefit of spatiograms over histograms in pearl image characterization and introduce the novel spatiogram-based metrics. Our experimental study results are presented and discussed in Section 3. Finally, some concluding remarks are given in Section 4.

2. SPATIAL FEATURES OF PEARLS IN PAINTINGS

For studying the images of jewels, it is essential to quantify the distinctive features that evoke visual impression of the jewel-like luster and sheen. In *The Ghent Altarpiece*, pearls are often characterized by a blurry highlight as a mirror image of the light source and a fine glowing line at the other side indicating the delicate sheen emanating from the surface [3]. For illustration, see the pearls in Fig. 2 (a) and (b), or the top left pearl in Fig. 4.

Digital image histograms can be used to discriminate between different materials in the scene: glass, wood, metal, and so on. However, histograms only characterize global intensity distribution in the image without capturing spatial relations between the image elements (pixel values).

The so-called *spatiogram* representation of the image data [4], adds to the histogram the spatial information about the data. We will show in this paper that various spatiogram features can be used to indicate more material properties (e.g. light reflectance or smoothness of the surface) but also those of the background. The details are explained later in this section.

2.1. Spatiogram and spatiogram similarity metric

In general, a spatiogram S is determined by three components [4]: the histogram bin count, c_b ; the spatial mean, $\mu_b = (\mu_{x,b}, \mu_{y,b})$; and the spatial covariance, $\Sigma_b = (\sigma_{xx,b}^2, \sigma_{yy,b}^2)$. Similar as with histograms, all three spatiogram components are computed for a set of bins, identified by index $b \in \{1, \dots, B\}$. To enable comparison between regions of different sizes, all spatial coordinates need to be normalized to the same range. In our experiments, this range is $[-1, 1]$. Visualization of multidimensional spatiogram data is non-trivial and, to our knowledge, it has not been addressed so far. We introduce here a spatiogram visualization with three types of plots, see Fig. 5: (S1) connected centers of bins, μ ; (S2) μ -positioned counts of bins (c -wide circles); and (S3) μ -positioned variances of bins (x and y error bars, respectively, $\pm\sigma_{xx}$ and $\pm\sigma_{yy}$ long). In all plots, the color identifies the bin, b . In Fig. 5, rows 2 and 3 illustrate the ability of spatiogram to capture the difference between two images even when their histograms are exactly the same.

Let $S = (c, \mu, \Sigma)$ and $S' = (c', \mu', \Sigma')$ denote two spatiograms, each with B bins. Using $\mathcal{N}(\mathbf{m}; \mu, \Sigma)$ to represent a normalized Gaussian evaluated at \mathbf{m} , we can write the spatiogram similarity measure as follows [5]:

$$\rho = \sum_{b=1}^B \sqrt{c_b c_{b'}} \left[8\pi |\Sigma_b \Sigma_{b'}'|^{\frac{1}{4}} \mathcal{N}(\mu_b; \mu_{b'}', \hat{\Sigma}_b) \right], \quad (1)$$

where $\hat{\Sigma}_b = 2(\Sigma_b + \Sigma_{b'}')$. The similarity score is $0 \leq \rho \leq 1$ and comparing any spatiogram to itself yields $\rho = 1$. But, the value of ρ cannot tell us about the specific details that contribute to $\rho < 1$. Therefore, we search for additional metrics for our analysis.

2.2. Spatiogram matching based on bin-similarity

In order to better understand the relation between the visual appearances of pearls and the properties of their spatiograms, we developed an algorithm to match the spatiogram of a given pearl image to that of a reference pearl. We refer to the process as *indirect spatiogram matching* and to the resulting image as *matched image*. The matching can be done using a kind of Markov Chain Monte Carlo (MCMC) sampler. This means: at each step, choose a pair of pixels randomly and swap their values if the change contributes to the increased spatiogram similarity, or otherwise accept the change with a certain probability. When all the sites are visited in this way, one iteration is completed and the number of iterations depends on the desired stopping criterion. In practice, we apply first histogram matching and then we apply the MCMC sampler sequentially bin-by-bin. We define a stopping criterion in terms of the required bin similarity. In particular, we use the symmetrized Kullback-Leibler (SKL) divergence between two model Gaussians with given means and covariances, $\mathcal{N}_b(\mu_b, \Sigma_b)$ and $\mathcal{N}_{b'}(\mu_{b'}, \Sigma_{b'})$. Note here that the means and covariances of the bins are spatial and not intensity based. The two bins are considered similar enough when the SKL divergence between their model Gaussians drops below a predefined threshold. Finally, we revert to the original histogram, by applying the reverse of the initial histogram matching operation. This step preserves the original “color palette” (intensity range) chosen by the artist.

2.3. New spatiogram metrics

By comparing the spatiograms of the pearls in paintings to those of their altered images matched to other pearls, we found four new metrics that characterize some interesting features of the pearl images.

Table 1. New spatiogram metrics for pearls images

Symbol	Name	Definition
M1	Mean(D)	$\frac{1}{N} \sum_i D_i, \quad i = 1, \dots, B-1$
M2	Var(D)	$\frac{1}{N} \sum_i (D_i - M1)^2$
M3	R_x	$\max_i \mu_{x,i} - \min_i \mu_{x,i}$
M4	R_y	$\max_i \mu_{y,i} - \min_i \mu_{y,i}$

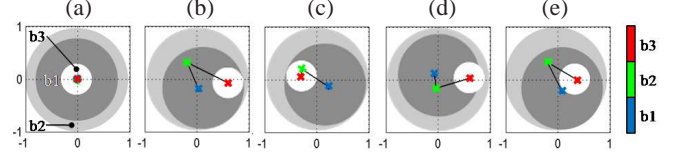


Fig. 1. Test images to illustrate the properties of M1-M4 (see text).

The proposed metrics are derived from the centers of spatiogram bins, μ_i , and their distances, D_i . Especially, we define the distance between the centers of the adjacent bins as the Euclidean distance: $D_i^2 = \mu_i^2 - \mu_{i+1}^2$ where $\mu_i = (\mu_{x,i}, \mu_{y,i})$ and $i = 1, \dots, B-1$. The new metrics M1 to M4 are summarized in Table 1. For illustration of their meanings, we create simplified model images shown in Fig. 1. In these synthetic pearls, we limit the number of bins to three: the area of bin b3 corresponds to the often observed mirror image of the light source, b2 depicts the main surface of the pearl, and b1 represents the glowing sheen usually present against the outline of the pearl (coming as a reflection of light from the background) [6].

The M1 and M2 metrics, respectively, are the mean and the variance of the D_i . The M1 captures the (circular) symmetry of the pearl area: the smaller M1 the higher the symmetry, suggesting potentially the less sharp angle between the light source and the pearl surface. For example, among pearls (a)-(c) in Fig. 1, M1 is the smallest for (a) and the largest for (b). The next metric, M2, relates to the uniformity of “distances” between different bin areas, or the impression of the surface smoothness. The M2 of pearl (e) is smaller than that of (d), for example, where the b2 and b3 areas intersect making an abrupt transition and diminishing smoothness of the surface.

The M3 and M4 metrics are the ranges R_x and R_y of bin centers in x - and y -direction, respectively. These two metrics tell us about (dominant) orientation of the asymmetry in the pearl, if any. For example, if a blurry highlight representing a mirror image of the light source would be further from the central vertical axis of the pearl (the sharper angle between the light source and the pearl surface), we would expect larger R_x compared to the case where this highlight is more centered on the pearl area (see pearls (b) and (d) versus (c), (e) and (a) in Fig. 1). Moreover, the glowing sheen usually present against the outline of the pearl, is often larger against a light-reflecting background [6]. This effect is frequently coupled with the larger circular asymmetry of the bin areas, like for example in Fig. 1 (e) where both x - or y -asymmetry exist. Hence, the larger ranges of bin centers can be an indication not only of the pearl properties itself but of the pearl background as well.

3. EXPERIMENTAL RESULTS

The results presented in this section are obtained for digital photographs of the considered paintings acquired either by the professional photographers or by amateurs, often in a non-controlled and non-uniform image acquisition conditions. Given the difficulty of



Fig. 2. Pearls in *The Ghent Altarpiece*, details from: (a) *God the Father*, (b) *Singing Angels*, (c) and (d) *The Holy Hermits*.

getting access to this kind of images, some of the experiments could only be performed for a limited set of pearls.

3.1. Pearl image processing system

As pre-processing, our experimental setup includes automatic pearl detection and registration. For pearl detection, we use the Hough transform [7], iteratively for a set of radii of interest. To reject false detections, for smaller pearls we also use a set of features that characterize painted pearls (the angle of reflection, smoothness and mean gray value). The images of extracted pearls are transformed to HSV color space and further on only the Value (V) channel is used. To eliminate concerns about the influence of cracks to the proposed pearl analysis, we performed crack detection followed by crack inpainting and our results (not shown here) suggest that spatiograms of V-pearl images are little sensitive to cracks. The last preprocessing step is the registration of the pearl images to the “reference” pearl (one arbitrarily selected pearl from the considered set). The registered pearls are then subject to the spatiogram analysis using the numerical metrics described in Section 2.

3.2. Pearls in *The Ghent Altarpiece*

Fig. 2 shows four details with pearls from the polyptych panel *The Ghent Altarpiece* by the Van Eyck brothers. We assess the similarity of different pearls using the spatiogram similarity metric ρ from Eq.(1). The results for $B = 128$ bins are summarized in Fig. 3.

Based on these bar charts, several observations can be made. First, we find that larger pearls (from more prominent objects) are more similar than the smaller ones. In Fig. 2 (a), we observe the 51 larger pearls laying in the frame of the broach (Object 1) and the 70 smaller pearls on the coat, outside the broach (Object 2). In Object 1, approximately 80% of the pearls are similar to each other with as much as $\rho > 0.9$, contrasted to $\approx 50\%$ among the pearls from Object 2. Perhaps more interestingly, we measure that pearls of the similar size, like the largest 4 pearls from each detail (a) and detail (b), are fairly similar across different paintings, $\rho \geq 0.8$. Finally, our results for similarity between 21 glass beads from detail (c) and 9 wooden beads from (d), indicate that different materials are painted significantly different, $\rho > 0.9$ with less than 5%.

3.3. Quantifying features of pearls from different artworks

For the following analysis, we consider example representative pearls from each of the following art works: (Pearl 1) *God the Father* from the great Flemish masterpiece *The Ghent Altarpiece* painted by Hubert and Jan van Eyck in the XVth century, (Pearl 2) a copy by Charlotte Caspers (2010) of the *Angels Playing Music* from *The Ghent Altarpiece*, (Pearl 3) a copy by Jef Van der Veken (1945) of the stolen panel *The Just Judges* from *The Ghent Altarpiece*, and (Pearl 4) one of the masterpieces of Northern Renaissance art *Maria Maddalena Baroncelli* by Hans Memling (1470). In addition,

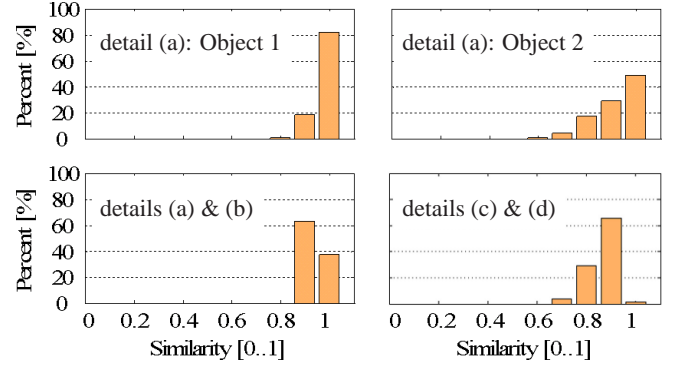


Fig. 3. Similarity of pearls from the details in Fig. 2 (see text).

we consider a set of 10 photographs of real pearls and select one example of those as well (Photo). The pearls are selected according to two criteria: (1) all similar in size (100 ± 30 pixels), and (2) representative spatiogram for a particular class (painting).

Fig. 4 shows the pearls together with their histograms and S1 spatiograms. Visually, Pearl 1 is most similar to Photo¹. This is also suggested by their high spatiogram similarity of $\rho \approx 0.90$, see Table 2. Note, however, that the ρ values in Table 2 do not exactly match the human-based similarity ranking. For example, ρ is in the same range for Pearl 4 and even Pearl 3 but these are visually less similar to Photo. The scoring of the proposed M-metrics does much better. By comparing these for the two pearls, we find that the relative distance between the metrics is highest for the M2. As discussed in Section 2.3, this suggests the difference in surface smoothness of the pearls. And indeed, this observation can be confirmed visually.

Fig. 5 illustrates the result of matching the spatiogram of Pearl 1 to Photo. We observe that visual appearance of the Pearl 1 after the matching is even more similar, if not almost the same as the one of Photo (see rows 1 and 3 in Fig. 5). The increase in similarity is also observed in the spatiograms (now $\rho^* \approx 0.95$), especially in the S1 plots, but again with no detailed characterization of the similarity. The values of the M1-M4, on the other side, nicely capture the features which contribute to the increased pearl similarity (e.g. $M2^* = 0.056$). This analysis is one more indication of the importance of S1 information in understanding the visually observed image features and the degree of realism of the visual appearance of the pearls. Remind that the image histogram is not affected by matching, only the spatial context is altered.

3.4. Pearls by different artists

In order to evaluate the potential of the proposed metrics to discriminate between pearls of different artists, we look back in *The Ghent Altarpiece* and compare the pearls by Van Eyck to those by Van der Veken. In particular, we select 20 Van Eyck’s pearls from Object 1 in the detail (a) of Fig. 2 whose spatiograms are most similar ($\rho > 0.8$) to (2) the 4 pearls from Van der Veken’s copy of the *Just Judges* panel from *The Ghent Altarpiece*. The mean and standard deviation of the M-metrics for these pearls summarized in Table 3 clearly indicate the difference of the two artists’ hands [8].

Finally, we show in Fig. 6 the results of matching pearls of other artists to the Van Eyck’s pearl. This kind of analysis can be of interest in, for example, studying the influence of the pearl characteristics on the visual impression of a painting.

¹Note that the type of light source is different in Pearl 1 and Photo.

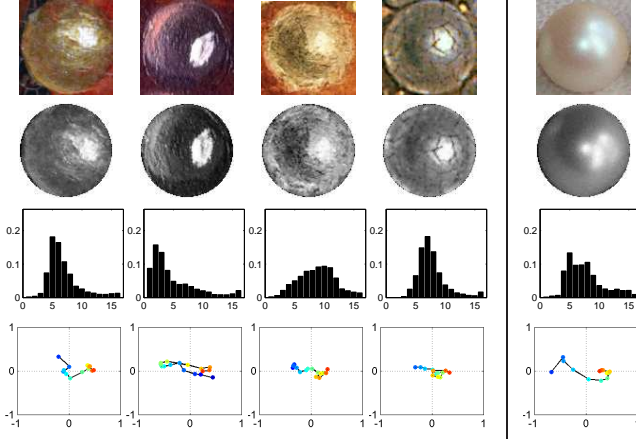


Fig. 4. Using S1 plots to characterize pearls. Left to right: Pearl 1, Pearl 2, Pearl 3, Pearl 4, Photo. Top to bottom: original RGB patch, registered HSV-V pearl, histogram, and S1 plot (B=16).

Table 2. New spatiogram metrics in characterizing pearls

	Pearl 1	Pearl 2	Pearl 3	Pearl 4	Photo
M1	0.231	0.185	0.122	0.146	0.210
M2	0.063	0.016	0.010	0.015	0.047
M3	1.358	0.998	0.692	0.777	1.347
M4	0.523	0.364	0.332	0.395	0.544
ρ_{photo}	0.899	0.640	0.867	0.901	1

Table 3. New spatiogram metrics in identifying artists

	Van Eyck	Van der Veken
M1	0.210 \pm 0.029	0.136 \pm 0.013
M2	0.055 \pm 0.019	0.009 \pm 0.002
M3	0.767 \pm 0.229	0.733 \pm 0.028
M4	0.899 \pm 0.210	0.457 \pm 0.139

4. CONCLUSIONS

The reported work focuses on developing the methods for quantifying properties of the pearls in paintings. Our proposed metrics built upon the spatiogram representation of the image data have been evaluated on a range of pearls, both painted or photographed ones. Overall, the observed high correlation between the new metrics and the visually observed image features makes them promising candidates for practical use in characterization of pearls in paintings. In particular, tentative applications for the proposed techniques include the following: (1) assisting art historians in better understanding the differences or similarities between different artists and their ways of painting pearls, (2) artist identification, and (3) forgery detection.

5. ACKNOWLEDGEMENTS

The Van Eyck images are based on photographic negatives (c-04,h-16,40-15) from the Dierickfonds made available to Ghent University by the family of the late Alfons Dierick. We thank Saint Bavo cathedral, Lukas Art in Flanders and the Dierickfonds for permission to

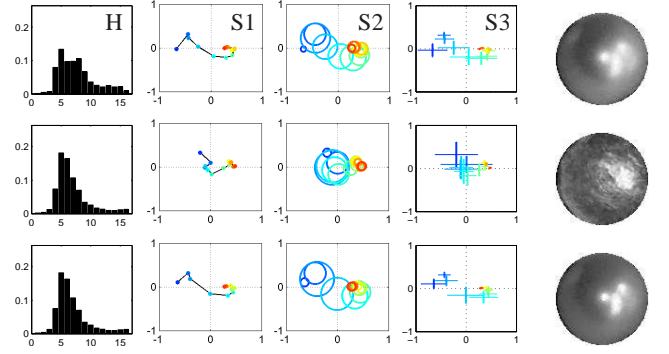


Fig. 5. Spatiogram matching (B=16). Photo pearl (top), Pearl 1 before (middle) and after (bottom) spatiogram matching to Photo. Left to right: histogram, S1, S2, S3, and registered HSV-V pearl.

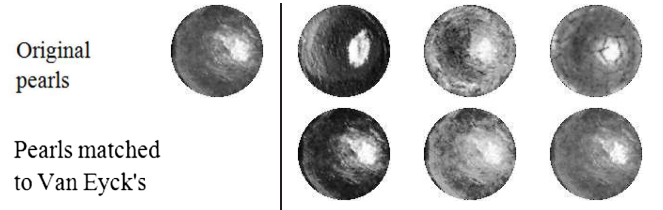


Fig. 6. Top (left to right): Pearls of Van Eyck, Caspers, Van der Veken, and Memling. Bottom: the upper pearls after spatiogram matching to the Van Eyck's pearl.

use these materials in this research report.

6. REFERENCES

- [1] R. Sinisgalli, *Alberti's "De Pictura". Il Nuovo De Pictura di Leon Battista Alberti, The New De Pictura of Leon Battista Alberti*, Edizioni Kappa, Roma, 2006.
- [2] M. C. Autin, A. Gonzalez-Palacios, and D. Scarisbrick, *Jewels in Painting*, Skira, Milano, Italy, 1999.
- [3] M. De Mey, *Jan van Eyck and the Representation of Glow*, in: *Anna De Floriani & Maria Clelia Galassi (eds.) Culture figurative a confronto tra Fiandre e Italia dal XV al XVII secolo*, Silvana Editoriale, Milano, 2008.
- [4] S. T. Birchfield and S. Rangarajan, "Spatigrams versus histograms for region-based tracking," in *IEEE CVPR*, 2005, vol. 2, pp. 1158–1163.
- [5] C. O. Conaire, N. E. O'Connor, and A. F. Smeaton, "An improved spatiogram similarity measure for robust object localisation," in *IEEE ICASSP*, 2007, vol. 1, pp. I-1069 –I-1072.
- [6] Farn, A. E. , *Pearls, Natural, Cultured and Imitation*, London, Butterworths, 1986.
- [7] R. O. Duda and P. E. Hart, "Use of the Hough transformation to detect lines and curves in pictures," *Commun. ACM*, vol. 15, pp. 11–15, 1972.
- [8] H. Verougstraete, R. Van Schoute, and T. H. Borchert, *Fake or not fake. Het verhaal van de restauratie van de Vlaamse Primitieven*, Ludion, Ghent-Amsterdam, 2004.